ISBN: 978-3-95450-231-8 ISSN: 2673-5490 doi: 10.18429/JACoW-IPAC2023-TUPM118

TAILORING TRANSVERSE BEAM CHARACTERISTICS WITH THE NEW CERN PS BOOSTER CHARGE-EXCHANGE INJECTION SYSTEM

E. Renner*, TU Wien, Vienna, Austria
S. Albright, F. Antoniou, F. Asvesta, H. Bartosik, C. Bracco, G. P. Di Giovanni,
B. Mikulec, T. Prebibaj, P. Skowronski, F. M. Velotti, CERN, Geneva, Switzerland

Abstract

A key aspect of the LHC Injectors Upgrade project is the connection of the PSB to the newly built Linac4 and the related installation of a new 160 MeV charge-exchange injection system. The new injection system was commissioned in winter 2020/21 and is now used operationally to tailor the transverse characteristics for the various beam types at CERN, such as high-intensity fixed target beams, LHC single bunch beams, and high-brightness beams for LHC.

This contribution outlines the different injection strategies for producing the various beam types and discusses the application of numerical optimization algorithms to adjust injection settings in operation efficiently.

INTRODUCTION

The Proton Synchrotron Booster (PSB) is the first synchrotron in the CERN injector chain. It is used for tailoring the wide range of transverse beam characteristics as requested by the various experiments, covering intensities within 10^{10}–10^{13} p+ per ring (ppr) and normalized transverse emittances within ≈0.7–9 µm. The PSB was upgraded during the Long Shut-Down 2 (LS2, 2019/20) as part of the LHC Injectors Upgrade project (LIU, [1]). A key aspect was connecting the PSB to the new H^- accelerator Linac4 [2] to increase the injection energy from 50 to 160 MeV and hence the relativistic $\beta\gamma^2$ by a factor of two. This allows doubling the beam brightness for the High-Luminosity LHC, while keeping space charge forces at the same level as pre-LS2.

To inject the 160 MeV H^- beam into the PSB, the conventional proton multi-turn injection had to be replaced with a new H^- injection system (Fig. 1, [3]). Its main components are the ≈200 µg cm^{-2} carbon stripping foil and a horizontal -81 mm orbit bump to direct the circulating beam towards the foil. Latter is created by a -46 mm injection chicane (BSW1-4 in Fig. 1) and a set of painting kicker magnets with variable field decay (nominal orbit bump of -35 mm).

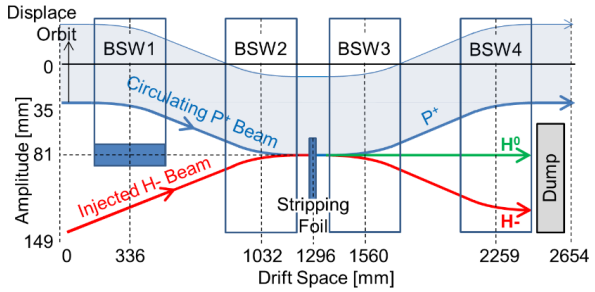

Figure 1: Schematic of the PSB H^- injection system [3].

* elisabeth.renner@tuwien.ac.at

USER-SPECIFIC INJECTION SCHEMES

To regulate the requested intensity, beam with $\epsilon_{x/y,\mathrm{n,L4}} \approx 0.3$ µm can be injected from Linac4 and accumulated in the PSB over $n_{\mathrm{inj}} = 1$–150 turns. The requested horizontal properties ($\epsilon_{x,\mathrm{n,PSB}} \approx 0.7$–9 µm) can be customized using horizontal phase space painting. In the PSB, this is facilitated by the piece-wise linear field decay of the painting kicker magnets [4], which can be configured through the time-amplitude knobs A_0, (A_1,t_1) and (A_2,t_2), as shown in Fig. 2. After t_2, the bump is designed to decay

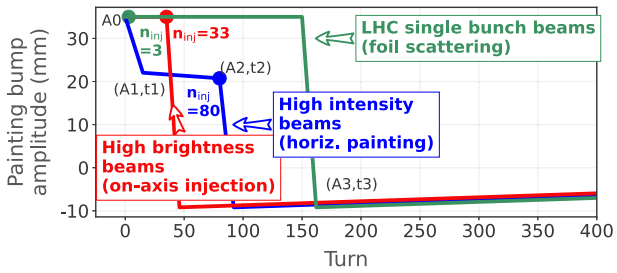

Figure 2: Painting bump decay for different users. The scatter markers indicate the end of injection for each user.

within 10–12 turns to the fixed amplitude A_3. This fast decay minimizes beam loss and degradation by removing the beam quickly from aperture limitations and the foil as soon as the injection process is finished. The vertical beam size can be tailored by configuring a constant vertical offset Δy between the injected and the circulating beam orbit.

The PSB provided and exceeded the challenging beam specifications for the various users already during the first operational year in 2021 [5]. This paper provides an overview of different injection schemes based on selected users.

On-axis Injection for High-brightness LHC Beams

The LHC requests beams with different intensities but maximized brightness for most variants. The LIU targets for the main operational variants in the PSB are 1.7×10^{12} ppr within $\epsilon_{x/y,\mathrm{n}} < 1.5$ µm (BCMS beam) and 3.52×10^{12} ppr within $\epsilon_{x/y,\mathrm{n}} < 2$ µm (LHC25 beam). In the baseline, we inject on-axis in both planes, i.e. without painting (red in Fig. 2). For this, the painting bump is kept at nominal amplitude while injecting over up to 35 turns (BCMS: 17, LHC25: 35). Subsequently, the bump decays immediately within ≈10 turns to prevent beam degradation due to foil scattering.

During beam commissioning, injection studies for LHC beams focused on assessing the sensitivity of the delivered beam properties to injection imperfections. These studies mainly concern LHC-type beams with low intensities, as for

ISBN: 978-3-95450-231-8 ISSN: 2673-5490 doi: 10.18429/JACoW-IPAC2023-TUPM118

beams with $\gtrsim 1 \times 10^{12}$ ppr the transverse emittance blow-up is dominated by space charge rather than injection errors.

During these studies, it was confirmed that the installed foils met the required specifications, ensuring that no significant brightness degradation is expected due to foil scattering [6, 7]. Moreover, Ref. [6] presents studies on the effect of steering errors at various intensities along the brightness curve, evaluating emittance growth and halo formation. Figure3 shows that beams with operational intensities, such as BCMS and LHC25, were not significantly disturbed by additional steering errors of $\Delta x, \Delta y \lesssim 2$ mm.

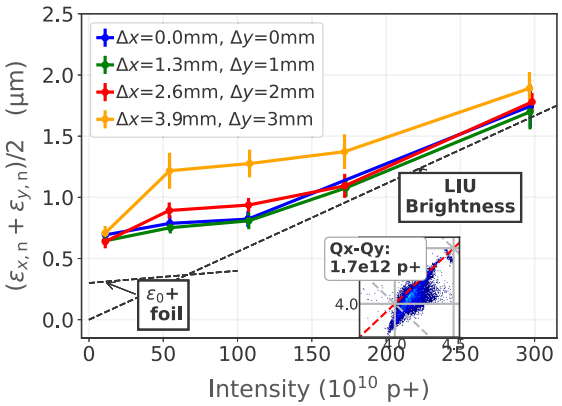

Figure 3: Impact of injection errors on the LHC brightness curve. The black line indicates the LIU brightness target. Note: Measurements performed in 2021, prior to several brightness optimizations, as presented e.g. in Ref. [8]. The measurement with 10×10^{10} ppr is obtained when injecting beam over a single turn, for which applying additional steering errors does not increase the core size but rather the halo.

Foil Scattering for LHC Single Bunch Beams

LHC Individual Bunch Physics beams (INDIV) have transverse emittances similar to LHC beams ($\epsilon_{x/y,\mathrm{n}} = 1$–$2\,\mu$m), but significantly lower intensities, i.e. 2–12×10^{10} ppr. A particular variant of such beams is used when calibrating the luminosity in the LHC with a Van der Meer scan [9], which requires a beam with large emittance, moderate intensity and a Gaussian beam profile. Pre-LS2, the production scheme for such beams relied on injecting similar intensities as for nominal LHC beams, i.e. 150–180×10^{10} ppr. As for nominal LHC beams, the high brightness caused a large incoherent space charge tune spread of $\Delta Q_{\mathrm{inc}} > -0.5$ during injection. The transverse emittances were established due to the consequent interaction with the integer resonances. Most of the beam was subsequently lost through a slow RF capture. Finally, intensity and emittance were fine-tuned with longitudinal and transverse shaving, respectively [10].

With the new injection system, these beams are produced without injecting and subsequently losing excessive intensity. $N_{\mathrm{p+}}$ =5.5–16.50 $\times 10^{10}$ ppr less than 10 % compared to pre-LS2, are injected over 1-3 turns from Linac4. As before, the intensity is then fine-tuned to 2–12×10^{10} ppr through longitudinal shaving. However, the incoherent space charge tune spread is now reduced to $\Delta Q_{\mathrm{inc}} \approx -0.1$ (during longitudinal filamentation) due to the decreased intensity and increased injection energy. Relying, as pre-LS2, on the integer resonances to provide $\epsilon_{x/y,\mathrm{n}} \approx 2\,\mu$m would require a working point close to the integer tunes, where small tune fluctuations could cause large emittance variations.

Instead, with the new injection system, it is possible to flexibly fine-tune the requested transverse emittance range without generating significant tails by combining controlled emittance growth from steering offsets and foil scattering (Fig. 4) [6]:

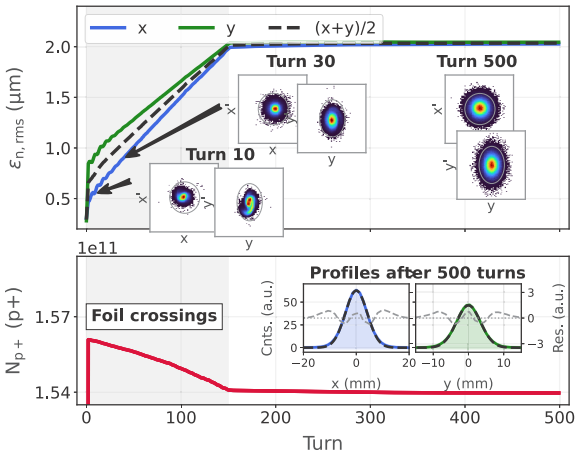

Figure 4: PyOrbit [11] simulations for tailoring INDIV beams using a combination of injection offsets and foil crossings (here $\Delta x = 2.5$ mm, $\Delta y = 3$ mm and $N_{\mathrm{F}} = 150$).

The injection bump can be kept at large amplitude over up to 150 turns, despite only injecting over 3 turns (green in Fig. 2). This allows to control the emittance growth due to Multi-Coulomb scattering, i.e.

$$\Delta\epsilon_{x/y,\mathrm{rms}} = \frac{\beta_{x/y} \cdot \langle\Theta^2\rangle}{2} \propto \beta_{x/y} \cdot N_{\mathrm{F}}, \qquad (1)$$

by directing the circulating beam a programmed number of N_{F} =3–150 times through the stripping foil. The expected r.m.s. angular spread due to foil scattering, $\sqrt{\langle\Theta^2\rangle} \propto \sqrt{N_{\mathrm{F}}}$, can be approximated using Moliere's formula [12] with the logarithmic correction for thin targets [13]. The blow-up is proportional to the local optics function $\beta_{x/y}$ and hence different horizontally and vertically. Transverse steering offsets are applied in addition to the injected beam to fine-tune ϵ_x and ϵ_y independently. The stochastic nature of the foil scattering-induced emittance growth yields close to Gaussian transverse beam profiles, also for non-Gaussian input distributions. Losses during this process are mainly attributed to large-angle single Coulomb scattering and are in the order of $\mathcal{O}(10^9)$ ppr, which is negligible compared to the $\mathcal{O}(10^{11})$ ppr lost when injecting high-intensity beams.

Analytic approximations and simulation studies for an operational working point (Q_x=4.17, Q_y=4.23 with $\beta_x \approx$ 5.7 m, $\beta_y \approx 4$ m, $\alpha_{x,y} \approx 0$ rad) suggest that injection settings in the range of $N_{\mathrm{F}} \approx$ 100–150, $\Delta x \approx$ 0-4 mm and $\Delta y \approx$ 2–4 mm are required to produce the requested beams with $\epsilon_{x/y,\mathrm{n}} = 1.5$–$2\,\mu$m (Fig. 4). These settings could be validated

ISBN: 978-3-95450-231-8 ISSN: 2673-5490 doi: 10.18429/JACoW-IPAC2023-TUPM118

experimentally, as described in Ref. [6]. For example, Fig. 5 compares vertical wire scanner measurements (solid lines) to simulations (dotted), when injecting 1.5×10^{11} ppr over 3 turns while varying Δy and N_F. The emittance $\epsilon_{y,n,fit}$ is obtained by performing a Gaussian fit of the beam core, the tails are quantified using $\sigma_{y,rms}/\sigma_{y,fit}$. The black scatter marker indicates that an INDIV beam with $\epsilon_{x/y,n} \approx 2\,\mu m$ and Gaussian profile could be operationally tailored in 2021 using $N_F = 150$, $\Delta x = 0$ mm and $\Delta y = 4$ mm.

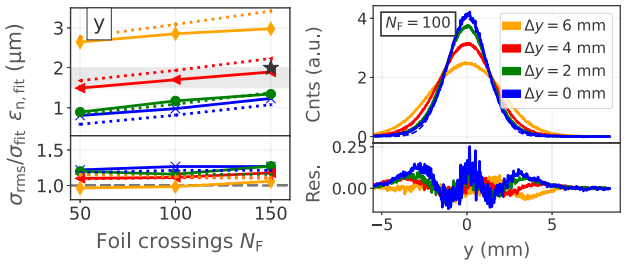

(a) Simulated (dotted) and measured (solid) emittances (top) and tails (bottom).

(b) Top: measured profiles for $N_F = 100$, compared to Gaussian fits (dashed). Bottom: residuals.

Figure 5: Vertical beam characteristics when producing INDIV beams with different PSB injection settings.

Painting for High-intensity Fixed Target Beams

Optimizing the injected beam distribution of high-intensity fixed target beams through phase space painting (blue in Fig. 2) is an ongoing research topic in several facilities, e.g. [14–18]. The aim is to meet the beam specifications at the target while minimizing space charge effects and losses. In the PSB, this technique is particularly relevant for the production of ISOLDE [19] beams, especially when pursuing efforts to increase their intensity to $\gtrsim 1 \times 10^{13}$ ppr in the future [20], while keeping the overall losses within a few percent. In 2021, simulations and measurements at operational intensities ($\approx 8.5 \times 10^{12}$ ppr) [6] showed that most losses (2–5 %) occurred along the cycle due to remnant 3rd and 4th-order resonances [20, 21], rather than during injection due to aperture bottlenecks (< 1%). Realistic variations of the painting functions affected both loss mechanisms, changing the total losses between ≈ 2–5 %. Generally, an optimized painting aims at fitting the beam into the machine acceptance while optimizing the space charge-induced tune spread at injection to compromise the interaction of particles in the beam core and tails with strong resonances. For the machine state in 2021, painting large initial emittances in both planes was not beneficial as it increased the number of particles with large transverse actions, which were consequently more sensitive to the excited 3rd and 4th-order resonances during the tune ramp. The overall losses were minimized when configuring a painting, which targets the transition from space charge to painting-driven emittance growth in the horizontal plane while injecting on-axis in the vertical plane [6].

AUTOMATING PHASE SPACE PAINTING

The proposed painting functions for the various users are sensitive to changes in the operational conditions or user requests. Finding solutions to efficiently and reliably adapt the injection settings based on pulse-per-pulse beam instrumentation feedback will push the operational performance of the PSB in the coming years. One promising approach for increasing operational efficiency is to automate the injection painting set-up using derivative-free numerical optimization algorithms, as also investigated for other applications in various facilities, e.g. [22–24]. In the PSB, an optimization framework for tailoring the high-intensity fixed target beam distributions was developed based on CERN's Generic Optimization Frontend and Framework (GeOFF, [25]). First optimization tests were successful in demonstrating the feasibility but also identified the challenges which must be overcome to make such a system operationally applicable [6]: The objective function features a high noise level (≈7 %), a flat minimum and is expensive to evaluate, with a new test cycle and hence acquisition available every ≈30 s. Performing systematic online tests with different algorithms to address these issues is not feasible as it would require thousands of acquisitions (limited beam time, machine drifts, ...). To overcome these limitations, we used supervised machine learning to train a data-driven surrogate model of the injection process [6]. For this, the random forest regressor [26] proved to be a robust method and is recommended for similar applications. This final model enabled tuning of the optimizer's hyperparameters and conducting systematic studies offline without requiring physical resources like beam time. The results emphasized the importance of appropriate noise reduction strategies. Out of the tested algorithms, the most promising were the solvers pyBOBYQA (with extension for noisy applications [27, 28]), adaptive Nelder Mead [29] and the surrogate-based optimizer pySOT [30]. These solvers were able to find acceptable painting settings in a 5 dimensional parameter space within $\mathcal{O}(100)$ acquisitions.

SUMMARY AND CONCLUSION

The new PSB H^- injection system at CERN offers a range of possibilities for tailoring the transverse characteristics of different beam variants. For LHC INDIV beams, a new injection scheme allows tailoring the transverse emittances by combining steering offsets and controlled emittance blow-up due to foil scattering. For LHC-type beams, which are injected on-axis, it was shown that no significant beam degradation for operational intensities is expected due to realistic injection errors. For high-intensity fixed target beams, it is essential to optimize the charge distribution during injection using phase space painting. Further, initial tests towards automating the injection painting setup using numerical optimization algorithms showed promising results. By training a supervised machine learning model of the injection process, it was possible to analyze the performance of various optimization algorithms in-depth offline.

ACKNOWLEDGMENTS

The authors would like to thank all teams involved in the PSB and Linac4 commissioning and operation, as well as V. Kain and N. Madysa, for the support with GeOFF.

ISBN: 978-3-95450-231-8 ISSN: 2673-5490 doi: 10.18429/JACoW-IPAC2023-TUPM118

REFERENCES

[1] J. Coupard *et al.*, "LHC Injectors Upgrade, Technical Design Report, Vol. I: Protons", CERN, Geneva, Switzerland, Rep. CERN-ACC-2014-0337, 2014.

[2] L. Arnaudon *et al.* "Linac4 Technical Design Report", CERN, Geneva, Switzerland, Rep. CERN-AB-2006-084, 2006.

[3] W. J. M. Weterings, C. Bracco, L. O. Jorat, M. Meddahi, R. Noulibos, and P. Van Trappen, "The New Injection Region of the CERN PS Booster", in *Proc. IPAC'19*, Melbourne, Australia, May 2019, pp. 2414–2417. doi:10.18429/JACoW-IPAC2019-WEPMP039

[4] L. M. C. Feliciano *et al.*, "A New Hardware Design for PSB Kicker Magnets (KSW) for the 35 mm Transverse Painting in the Horizontal Plane", in *Proc. IPAC'15*, Richmond, VA, USA, May 2015, pp. 3890–3892. doi:10.18429/JACoW-IPAC2015-THPF086

[5] V. Kain *et al.*, "Achievements and Performance Prospects of the Upgraded LHC Injectors", in *Proc. IPAC'22*, Bangkok, Thailand, Jun 2022, pp. 1610–1615. doi:10.18429/JACoW-IPAC2022-WEIYGD1

[6] E. Renner, "Commissioning of the New CERN PS Booster Charge Exchange Injection System: Optimising and Automating Transverse Phase Space Painting", Geneva, Switzerland, Rep. CERN-THESIS-2022-241, 2022.

[7] E. Renner *et al.*, "Beam Commissioning of the New 160 MeV H- Injection System of the CERN PS Booster", in *Proc. IPAC'21*, Campinas, Brazil, May 2021, pp. 3116–3119. doi:10.18429/JACoW-IPAC2021-WEPAB210

[8] T. Prebibaj *et al.*, "Injection chicane beta-beating correction for enhancing the brightness of the CERN PSB beams", in *Proc. HB'21*, Chicaco, USA, Sep. 2021, pp. 112-117. doi:10.18429/JACoW-HB2021-MOP18

[9] S. van der Meer "Calibration of the effective beam height in the ISR", CERN, Geneva, Switzerland, Rep. CERN-ISR-PO-68-31, 1968.

[10] H. Bartosik and G. Rumolo, "Production of single Gaussian bunches for Van der Meer scans in the LHC injector chain", CERN, Geneva, Switzerland, Rep. CERN-ACC-NOTE-2013-0008. 2013.

[11] A. Shishlo *et al.* "The Particle Accelerator Simulation Code PyORBIT", in *Proc. ICCS'15*, Reykjavík, Iceland, Jun. 2015, pp. 1272–1281.

[12] J.-B. Moliere, "Theorie der Streuung schneller geladener Teilchen I. Einzelstreuung am abgeschirmten Coulomb Feld", *Z. Naturforsch. A*, vol. 2, pp. 133-145, 1947. doi:10.1515/zna-1947-0302

[13] V. L. Highland, "Some Practical Remarks on Multiple Scattering", *Nucl. Instrum. Methods*, vol. 129, pp. 497-499, 1975. doi:10.1016/0029-554X(75)90743-0

[14] M.- Y. Huang *et al.*, "Study on the anti-correlated painting injection scheme for the Rapid Cycling Synchrotron of the China Spallation Neutron Source", *Nucl. Instrum. Methods*, vol. 1007, p. 165, 2021. doi:10.1016/j.nima.2021.165408

[15] H. Hotchi *et al.*, "Beam loss reduction by injection painting in the 3-GeV rapid cycling synchrotron of the Japan Proton Accelerator Research Complex", *Phys. Rev. ST Accel. Beams*, vol. 15, no. 15, p. 040 402, 2012. doi:10.1103/PhysRevSTAB.15.040402

[16] H. Hotchi *et al.*, "Effects of the Montague resonance on the formation of the beam distribution during multiturn injection painting in a high-intensity proton ring", *Phys. Rev. Accel. Beams*, vol. 23, no. 5, p. 050 401, 2020. doi:10.1103/PhysRevAccelBeams.23.050401

[17] W. Tao *et al.*, "Beam-loss driven injection optimization for CSNS/RCS", *Chin. Phys. C*, vol. 34, no. 2, pp. 218–223, 2010. doi:10.1088/1674-1137/34/2/012

[18] J. Holmes *et al.*, "Injection of a self-consistent beam with linear space charge force into a ring", *Phys. Rev. Accel. Beams*, vol. 21, no. 12, 2018. doi:10.1103/PhysRevAccelBeams.21.124403

[19] B. Jonson and K. Riisager, "The ISOLDE facility", *Scholarpedia*, 5(7):9742, 2010. doi:10.4249/scholarpedia.9742

[20] F. Asvesta *et al.*, "High Intensity Studies in the CERN Proton Synchrotron Booster", in *Proc. IPAC'22*, Bangkok, Thailand, Jun 2022, pp. 2056–2059. doi:10.18429/JACoW-IPAC2022-WEPOTK011

[21] F. Asvesta *et al.*, "Resonance Compensation for High Intensity and High Brightness Beams in the CERN PSB", in *Proc. HB'21*, Chicaco, USA, Sep. 2021, pp. 40–45. doi:10.18429/JACoW-HB2021-MOP06

[22] C. Xu *et al.*, "Bayesian optimization of the beam injection process into a storage ring", *Phys. Rev. Accel. Beams*, vol. 26, p. 034601, 2023. doi:10.1103/PhysRevAccelBeams.26.034601

[23] R. Ramjiawan *et al.*, "Design and operation of transfer lines for plasma wakefield accelerators using numerical optimizers", *Phys. Rev. Accel. Beams*, vol. 25, p. 101602, 2022. doi:10.1103/PhysRevAccelBeams.25.101602

[24] A. Scheinker *et al.*, "Online multi-objective particle accelerator optimization of the AWAKE electron beam line for simultaneous emittance and orbit control", *AIP Adv.*, vol. 10, p. 055320, 2020. doi:10.1063/5.0003423

[25] V. Kain and N. Madysa, "Generic Optimisation Frontend and Framework (GeOFF)", https://gitlab.cern.ch/vkain/acc-app-optimisation

[26] L. Breiman *et al.* "Random Forests", *Mach. Learn.*, vol. 45, pp. 5–32, 2001. doi:10.1023/A:1010933404324

[27] C. Cartis *et al.*, "Improving the Flexibility and Robustness of Model-Based Derivative-Free Optimization Solvers", *ACM Trans. Math. Software*, vol. 45, no. 3, p. 32, Aug. 2019. doi:10.1145/3338517

[28] C. Cartis *et al.*, "Escaping local minima with local derivative-free methods: a numerical investigation", *Optimization*, vol. 71, no. 8, pp. 2343-2373, 2022. doi:10.1080/02331934.2021.1883015

[29] J. A. Nelder and R. Mead, "A simplex method for function minimization", *Comput. J.*, vol. 7, no. 4, pp. 308–-313, 1965. doi:10.1093/comjnl/7.4.308

[30] D. Eriksson, D. Bindel, and C. A. Shoemaker, "pySOT and POAP: An event-driven asynchronous framework for surrogate optimization", *arXiv*, 2019. doi:10.48550/arXiv.1908.00420